Characterization of Damage Modes in Dental Ceramic Bilayer Structures

Yan Deng,*[,1] Brian R. Lawn,[1] Isabel K. Lloyd [2]

[1] Materials Science and Engineering Laboratory, National Institute of Standards and Technology, Gaithersburg, Maryland 20899

[2] Department of Materials and Nuclear Engineering, University of Maryland, College Park, Maryland 20742

Received 18 July 2001; revised 24 September 2001; accepted 26 September 2001

Abstract: Results of contact tests using spherical indenters on flat ceramic coating layers bonded to compliant substrates are reported for selected dental ceramics. Critical loads to produce various damage modes, cone cracking, and quasiplasticity at the top surfaces and radial cracking at the lower (inner) surfaces are measured as a function of ceramic-layer thickness. It is proposed that these damage modes, especially radial cracking, are directly relevant to the failure of all-ceramic dental crowns. The critical load data are analyzed with the use of explicit fracture-mechanics relations, expressible in terms of routinely measurable material parameters (elastic modulus, strength, toughness, hardness) and essential geometrical variables (layer thickness, contact radius). The utility of such analyses in the design of ceramic/substrate bilayer systems for optimal resistance to lifetime-threatening damage is discussed. © 2002 John Wiley & Sons, Inc. J Biomed Mater Res (Appl Biomater) 63: 137–145, 2002; DOI 10.1002/jbm.10091

Keywords: dental ceramics; elastic modulus; hardness; fracture; layer structures; material design; strength; toughness

INTRODUCTION

Laminate structures with brittle outer layers are important in biological systems such as shells, teeth, and prosthetic implants, as well as in a range of engineering applications. Brittle coating layers impart high wear resistance, biocompatibility, and chemical or thermal inertness to the composite structure. However, the lifetimes of such structures are generally limited by any one of a number of damage modes that may develop in the coating layer, especially under concentrated loading conditions.[1] Figure 1, showing the in vivo failure of an all-ceramic molar crown after 2 years, is an illustrative case in point. There is accordingly a need to develop test protocols for quantifying these modes in ceramic-based layer structures, in order to enable design and development of superior materials systems with longer lifetimes.

One such test protocol involves Hertzian testing with spherical indenters on model flat-surface structures, most commonly in single-cycle loading but also (to facilitate fatigue testing) in cyclic loading.[1,2] This test usefully simulates basic elements of occlusal function,[3–9] and so is clinically relevant in the characterization of potential ceramic materials for dental crowns. Although it is just one of many approaches that might be adopted to investigate damage modes in dental materials, Hertzian testing offers unique simplicity in testing and analysis. In monolithic ceramics, such testing has been used to distinguish two competing near-contact damage modes: *brittle mode*—in fine-grain, high-strength polycrystalline ceramics (and glasses), classical conelike tensile cracks initiating from the upper surface;[1,10–12] *quasiplastic mode*—in coarse-grain, high-toughness ceramics, distributed shear-microcracks initiating within a subsurface yield zone.[7,13–15] Analogous tests on flat ceramic layers bonded to dentinlike soft substrates[16–22] indicate a third mode, *radial cracking* at the inner surface (i.e., at the ceramic-layer/substrate interface), driven by undersurface tension from flexure of the ceramic layer on the soft support. In this mode, the Hertzian contact may be regarded simply as a generic applied load which can induce ceramic plate flexure and hence initiate inner surface radial cracks—specific details of the loading are not critical. These cracks are most relevant in the context of failure of all-ceramic crowns, because they can occur at

Information on product names and suppliers in this article does not imply endorsement by NIST.

*Ph.D. student, Department of Materials and Nuclear Engineering, University of Maryland, College Park, MD 20742-2115

Correspondence to: Brian R. Lawn, Materials Science and Engineering Laboratory, Bldg. 223, Room B309, National Institutes of Standards and Technology, 100 Bureau Dr., Mail Stop 8500, Gaithersburg, MD 20899-8500 (e-mail: brian.lawn@nist.gov).

Contract grant sponsor: U. S. National Institute of Dental Research

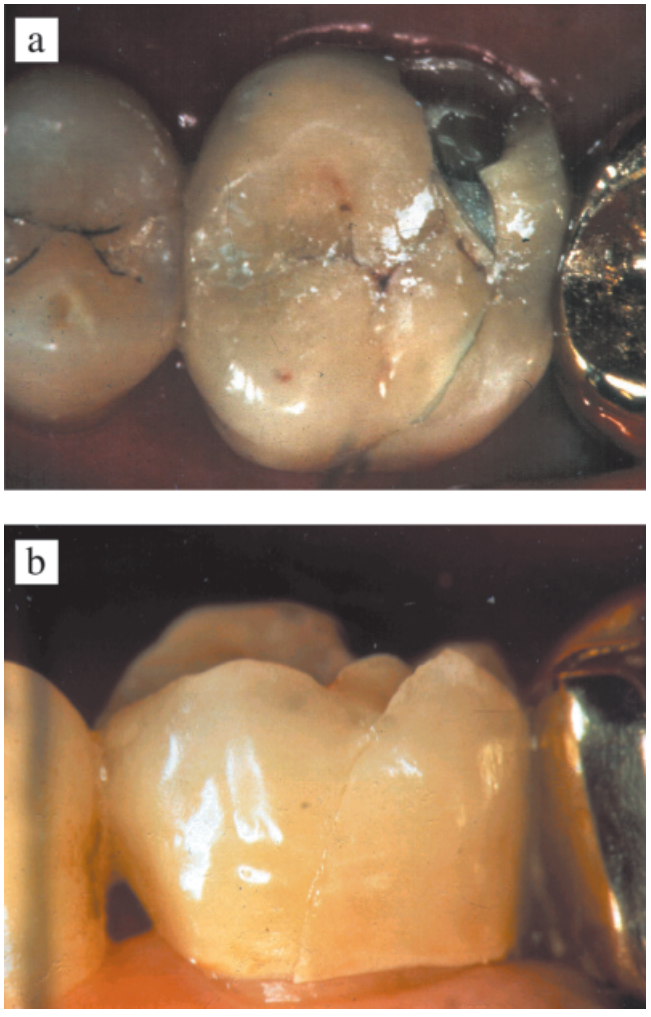

Figure 1. Failure of all-ceramic molar crown after 24 months: (a) occlusal view, (b) buccal view. Courtesy S. Scherrer.

relatively low loads and spread over long lateral distances. They are believed to be the source of failures such as that in Figure 1.[9] Radial cracks may remain entirely subsurface prior to the point of failure and therefore pass undetected in opaque layer materials. Explicit relations for the critical load for each of the above damage modes in terms of basic materials properties and other variables are now available for quantitative analysis.[2,23]

In dentistry, there has been a significant move away from traditional porcelain-fused-to-metal crowns toward all-ceramic crowns, for aesthetic as well as for the durability elements alluded to above.[9] Ideally, one would like to be able to replace severely damaged tooth enamel with a single monolithic ceramic possessing both aesthetics *and* durability. However, development of monolithic all-ceramic crowns with the capacity to withstand typical biting forces of 100–200 N over cuspal radii 2–4 mm for up to 10^6 chewing cycles or more per year[7] over acceptable lifetimes has proved elusive.[24] In reality, ceramic-based crowns are fabricated as layer structures with aesthetic but weak veneer porcelains on stiff and strong ceramic support cores, with a minimum combined thickness $\approx$ 1.0–1.5 mm.[6] Nevertheless, the ideal of a single brittle layer on a compliant support marks an important first step in understanding prospective crown behavior, and in any case provides data input for ensuing design of complex trilayer systems.[25]

Application of Hertzian contact testing to the evaluation of ceramic materials for dental crowns is a primary goal of the present study. This article reports on single-cycle Hertzian indentation experiments on model flat bilayer systems consisting of selected dental ceramic layers bonded to compliant polycarbonate substrate bases. The choice of polycarbonate as base material is to facilitate in situ observation of the all-important radial cracking mode during actual contact.[21] Critical loads to initiate each damage mode are thereby measured over a broad range of ceramic layer thicknesses. The critical load data are compared with predictions from basic fracture mechanics relations, using independently measured material parameters (elastic modulus, strength, hardness, and toughness) and key geometrical dimensions (layer thickness, sphere radius). Such results may be used as a basis for material characterization and design parameters for more complex crown and other biomechanical structures.

MATERIALS AND METHODS

Contact Testing and Damage Modes

Basic details of the Hertzian contact test used in this study are shown in the schematic of Figure 2. Indentations are made in normal loading with the use of tungsten carbide (WC) spheres. Generally, single load–unload cycles are applied at each contact site in air at fixed displacement rates, with typical contact durations $\approx$100 s,[14,26] although these conditions can be systematically varied to study fatigue and rate effects in aqueous environments.[27–29]

Whereas a certain amount of information on damage modes can be realized from simple inspections of surface indentation sites, it is generally necessary to explore the

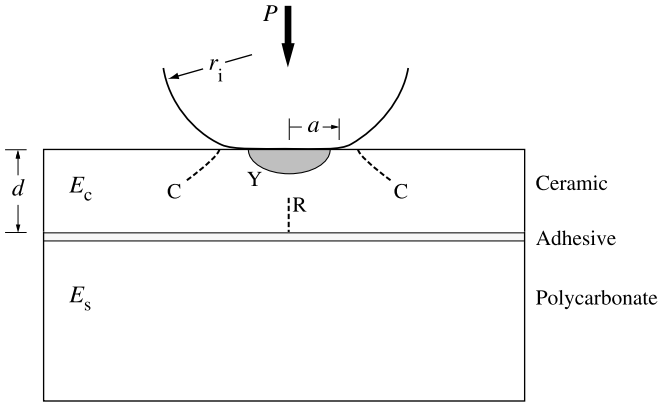

Figure 2. Schematic of brittle layer of thickness *d* bonded with thin adhesive to a thick compliant substrate, indented with sphere of radius r_i at load *P*. Damage modes: surface cone cracks (C); quasi-plastic yield zone (Y); inner-surface radial cracks (R).

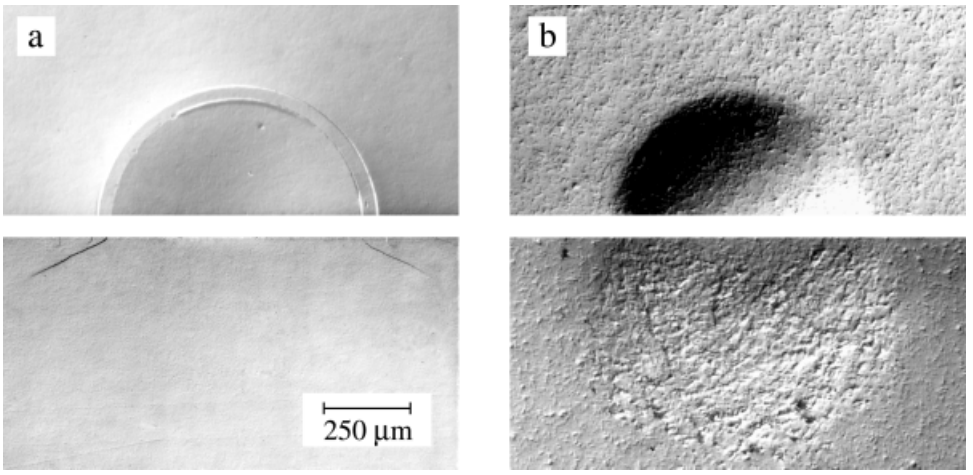

Figure 3. Top and section views of damage in bonded-interface specimens of (a) fine-grain and (b) coarse-grain micaceous glass–ceramic, from indentation with WC sphere of radius r_i = 3.18 mm at load P = 1000 N. From Reference 31.

subsurface regions as well. One way of accomplishing this is to employ a bonded-interface technique in which specimens are split and rejoined prior to indentation, and the ensuing damage is viewed in Nomarski illumination after gold-coating the separated surfaces.[26,27] Figure 3 shows micrographs of sphere-indentation damage from a WC sphere of radius r =3.18 mm at load P = 1000 N (cf. nominal biting force of 100–200 N) in two monolithic micaceous glass–ceramics formed from the same original glass composition but with two different grain sizes (controlled by heat treatment).[26,30,31] This glass composition is the basis for the (now discontinued) dental ceramic Dicor developed by Corning,[32] with a microstructure scale intermediate between those in Figures 3(a) and 3(b). The fine-grain material [Figure 3(a)] shows dominant cone cracking, the coarse-grain material [Figure 3(b)] shows dominant quasiplasticity. Both damage modes evolve further in cyclic loading:[33] the brittle mode by slow extension of the cone crack; and the quasiplastic mode by relatively rapid microcrack coalescence, leading ultimately to formation of dangerous subsurface radial cracks. These latter cracks can seriously degrade the strength of the ceramic, especially in cyclic loading in aqueous environments.[33–38] Quasiplasticity-induced radial cracks may develop in even the most brittle ceramics, including glasses and dental porcelains.[33,38,39]

Analogous contact-induced damage in a bonded-interface bilayer specimen is illustrated in Figure 4, for a fine-grain micaceous glass–ceramic coating bonded with a thin (≈ 10 μm) interlayer of dental cement to a filled-polymer composite substrate.[20] Elastic moduli of the coating and substrate materials are comparable to those of tooth enamel and dentin. The contact load P = 250 N used is substantially lower than that in Figure 3, and much closer to our nominal biting force of 100–200 N. Traces of conelike cracks are evident, although the cone diameters are considerably wider than those in monoliths [cf. Figure 3(a)]. Upward-extending radial cracks are now also evident.[16,21,40] These changes in crack configuration are attributable to enhanced flexure of the ceramic plate on the softer polymeric-based substrate, with

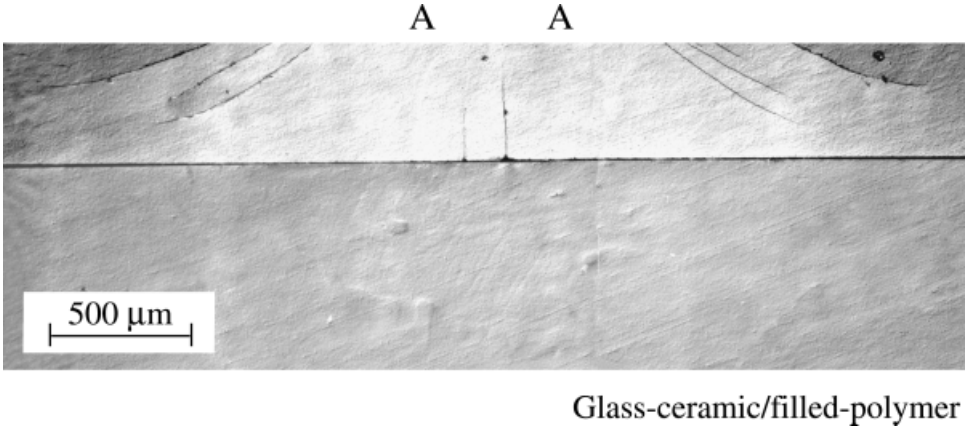

Figure 4. Section views of cracking in flat ceramic/substrate bilayers, from bonded-interface specimen of glass–ceramic/filled-polymer, ceramic thickness d = 0.45 mm, WC sphere indenter r_i = 3.18 mm at P = 250 N. From Reference 20.

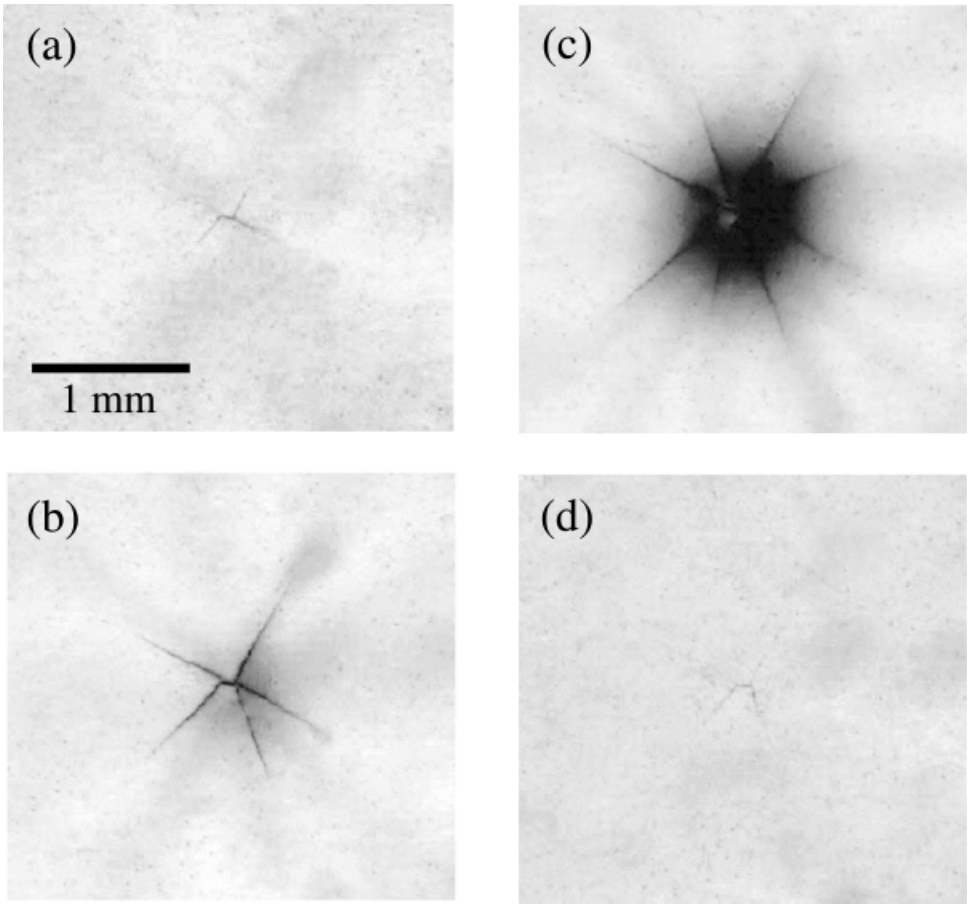

Figure 5. In situ views of radial crack sequence at lower as-polished surface of alumina coating, thickness $d = 0.15$ mm, on polycarbonate substrate, from indentation with WC sphere, $r_i = 3.96$ mm. Loading half cycle, (a) $P = 15.1$ N, (b) $P = 35.1$ N, (c) $P = 56.6$ N, and (d) $P = 0$ N (unloaded). From Reference 23.

characteristic development of a primary tensile stress maximum at the lower coating surface and secondary maximum at the outer shoulders of the top surface (along with simultaneous suppression of the Hertzian tensile maximum at the contact circle).[21]

Although bonded-interface and other postindentation sectioning specimens are useful in identifying damage modes, they are limited in their capacity to quantify critical loads and to determine of out-of-plane crack geometries. Acoustic detection may be used to detect the onset of cracking in some noisy opaque ceramics, but even then it is not always easy to determine which crack forms first, or how the different cracks evolve. For these reasons, model crown/dentin-layer structures have been constructed with the use of representative transparent substrates to allow direct in situ viewing of the ceramic undersurface during loading and unloading.[21,22] Figure 5 is an illustrative example for a relatively thin ($d = 155$ μm) glass-infiltrated dental-alumina plate bonded to a thick (12.5 mm) polycarbonate substrate with an ultrathin (≈ 10 μm) interlayer of epoxy adhesive.[23] The sequence shows initiation, expansion, and closure of radial cracks during the loading–unloading cycle. Comparative in situ side views in specimens with transparent glass coating layers[21] indicate extensive lateral propagation of the radial cracks over distances several times the ceramic thickness, with penetration to the upper surface only at very high loads (i.e., well above those represented in Figure 5). Such cracking, even in its early stages, severely compromises the specimen integrity, and can be considered as signaling an effective end to useful lifetime.

Interestingly, delamination failures are not commonly observed in the experimental arrangement of Figure 2,[20,23] despite the weak interlayer interfaces. When delamination does occur, usually at very high loads, it is usually preceded by radial fracture.

Fracture Mechanics Relations

Closed-form relations expressing critical load relations for cone-crack (C), quasiplasticity (or yield, Y), and radial-crack (R) damage modes in terms of basic materials properties and key geometrical variables have recently been reported.[2,15,23,41] Begin by defining an effective sphere radius r and an effective coating modulus E:[15]

$$1/r = 1/r_c + 1/r_i \tag{1a}$$

TABLE I. Properties of Dental Materials Used in this Study[a]

Material	Name	Supplier	Modulus (GPa)	Hardness[b] (GPa)	Toughness (MPa · $m^{1/2}$)	Strength (MPa)
Ceramics						
Porcelain	Mark II	Vita Zahnfabrik	68	6.2	0.9	100
	Empress	Ivoclar	67	5.6	1.4	120
Glass–ceramic	Empress II	Ivoclar	104	5.5	2.9	320
Alumina (glass-infiltrated)	InCeram	Vita Zahnfabrik	270	12.3	3.0	550
Zirconia (glass-infiltrated)	InCeram	Vita Zahnfabrik	245	13.1	3.5	440
Zirconia (Y-TZP)	Prozyr	Norton	205	12.0	5.4	1450
Enamel	Tooth	—	94	3.2	0.8	—
Substrates						
Filled polymer	Charisma	Hereaus	10	0.8	—	—
Polycarbonate	Hyzod	AI Plastics	2.3	0.15	—	—
Epoxy adhesive	RT Cure	Master Bond	3.5	0.9	—	—
Dentin	Tooth	—	20	0.6	3.1	—
Indenter						
Tungsten carbide	Kennametal	J&L Industrial	614	19	—	—

[a] Data courtesy I.M. Peterson, Y.-W. Rhee, J. Quinn, H. Xu. Experimental uncertainties estimated at 5% in E, 10% in H, 15–20% in T, 15–20% in σ_F.
[b] Indentation hardness, $H = 2P/a^2 = 1.078H_V$, a = indent diagonal.

$$1/E = 1/E_c + 1/E_i \tag{1b}$$

where subscripts c and i refer to ceramic and indenter materials, respectively. Then the key critical load relations have the following forms.

(i) *Cone cracks* initiate from the top surface outside the contact circle, where the Hertzian tensile stress is maximum.[10,11] The crack first grows downward as a shallow, stable surface ring, resisted by the material toughness T (K_{IC}), before popping into full cone geometry at load

$$P_C = A(T^2/E)r \tag{2}$$

with $A = 8.6\times10^3$ from fits to data from monolithic ceramics with known toughness.[15]

(ii) *Quasiplasticity* initiates when the maximum shear stress in the Hertzian near field exceeds $Y/2$, with yield stress $Y \approx H/3$ determined by the material hardness H (load/projected area, Vickers indentation).[42] The critical load is

$$P_Y = DH(H/E)^2r^2 \tag{3}$$

with $D = 0.85$ from fits to data for monolithic ceramics with known hardness.[15]

(iii) *Radial cracks* initiate spontaneously from a starting flaw at the lower ceramic surface when the maximum tensile stress in this surface equals the bulk flexure strength σ_F, at load

$$P_R = B\sigma_F d^2/\log(E_c/E_s) \tag{4}$$

with d the ceramic layer thickness and $B = 2.0$ from data fits to well-characterized ceramic-based bilayer systems.[23]

Thus, given basic material parameters, one can in principal make a priori predictions of the critical loads for any given bilayer system. Note that P_C and P_Y in Eqs. (2) and (3) are independent of layer thickness d, whereas P_R in Eq. (4) is independent of sphere radius r. These relations, within the limits of certain underlying assumptions, have been verified for model ceramic/substrate bilayer systems.[2,23]

Materials Used in this Study

The present study considers a range of dental ceramics used in crown preparation, either currently or in the recent past. These are listed in Table I, along with basic material properties evaluated with the use of routine materials testing procedures: elastic modulus E (from ultrasonic techniques); hardness H (from Vickers indentation, as load/projected area[42,43]); toughness T (K_{IC}, from Vickers indentation crack measurements[44]); and strength σ_F (four-point or biaxial flexure, polished surfaces). Table I includes data for indenter and substrate materials, as well as for tooth enamel and dentin. It should be emphasized that these data are susceptible to batch-to-batch variations, depending on the material source and specimen preparation, so the values cited should not be regarded as more than representative of any material type.

Accordingly, bilayers were prepared as polished ceramic plates of thickness $d = 100$ μm to 7 mm bonded with epoxy adhesive to transparent polycarbonate substrates of thickness 12.5 mm, for in situ viewing during indentation. The specimens were clamped during bonding, resulting in an adhesive interlayer ≈ 10 μm thick. Because the adhesive has similar modulus properties to that of the substrate, the interlayer thickness is not considered an important parameter in the bilayer structures.[21]

Critical Load Measurements on Test Bilayers

The bilayer specimens thus fabricated were subjected to indentation with WC spheres of radius $r = 3.96$ mm mounted

into the crosshead of an Instron testing machine (Instron Model 1122, Instron, Canton, MA), at a fixed crosshead speed 0.1 mm/min, in air. Radial crack initiation and evolution was monitored in situ from below the contact through the transparent adhesive/polycarbonate sublayer with the use of an optical zoom microscope (Optem, Santa Clara, CA) in conjunction with a videotape recorder.[21,22,45] Means and standard deviations for the critical load P_R for radial cracking were determined directly from the videotape, for a minimum of five indentations at each load condition.

An a posteriori procedure was used to determine the critical loads for cone cracking and quasiplasticity in the ceramic layers.[7] Rows of indentations were made on each ceramic surface at incrementally increasing peak loads, and the indented outer surfaces were gold coated and examined in Nomarski illumination. Mean and uncertainty bounds for P_C were determined from the loads over which surface ring cracks first appeared as incipient shallow arcs (lower limit) and were fully formed (upper limit), for a minimum of 5 indentations at each load. Values for P_Y were similarly determined as the load ranges over which residual surface impressions were completely undetectable and were clearly visible.

RESULTS AND ANALYSIS

Critical Loads

Figure 6 shows results of critical load measurements using spheres of radius $r_i = 3.96$ mm on flat ceramic/polycarbonate bilayers as a function of coating layer thickness d. The data points represent critical loads for first damage: at large d, unfilled symbols, either cone cracking (P_C) or quasiplasticity (P_Y), whichever occurs first (quasiplasticity in all cases except Mark II porcelain); at small d, filled symbols, radial cracking (P_R). The lines are corresponding predictions from Eqs. (2)–(4), inserting $r_c = \infty$, $r = r_i$ into Eq. (1) and using material parameters from Table I. As expected, the P_C and P_Y data are insensitive to d, whereas the P_R data are highly sensitive, covering a range of more than two orders of magnitude.

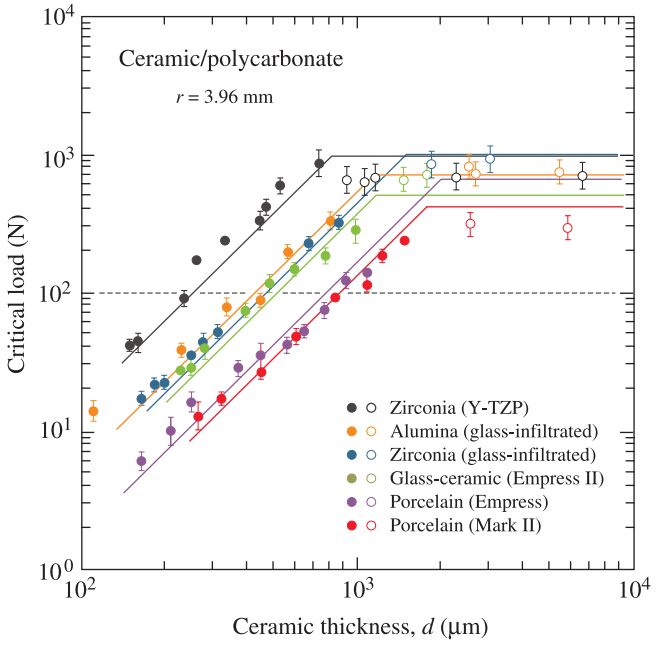

Figure 6. Critical loads for first damage in ceramic/polycarbonate bilayers as function of coating thickness d, for indentation with WC spheres of $r_i = 3.96$ mm. Solid symbols are P_R data, open symbols P_C or P_Y data. Error bars are uncertainty bounds. Solid lines are theoretical predictions for radial (inclined lines) and cone cracking and quasiplasticity (horizontal lines). Dashed line is nominal operational load $P_m = 100$ N for dental function.

Notwithstanding the broad agreement between experimental data and theoretical predictions, some deviations are evident. In particular, the exponent in a power-law $P_R \propto d^m$ data fit would appear to be a little less than the ideal $m = 2$ in Eq. (4).[21] However, in the context of the wide range of d values covered in Figure 6, deviations of a factor of 2 or more may not be so consequential.

Of special relevance to dentistry is the tendency for the data in Figure 6 to fall into three main groups in the low-thickness, radial crack region. The lowest-strength group consists of the aesthetic porcelains (Mark II, Empress), with glass-infiltrated core ceramics (Vita alumina and zirconia) plus strengthened glass–ceramic (Empress II) intermediate, and fully dense zirconia (Y-TZP) highest.

Design Considerations

The above results provide a starting point for designing ceramic-based bilayer structures. To avoid any form of damage in a given material system, it is necessary to operate below the appropriate bounding data envelope in Figure 6. Or, given a nominal maximum operational load P_m, it is necessary to satisfy two sets of requirements: first, that P_m remains below the lesser of P_C and P_Y, which in turn implies a minimum sphere radius r_C or r_Y in Eqs. (2) and (3); and second, that P_m remains below P_R, which implies a minimum thickness d_R in Eq. (4). Suppose the operational load is $P_m = 100$ N, indicated by the horizontal dashed line in Figure 6. Then for the ceramic/polycarbonate bilayers and WC sphere radius ($r = 3.96$ mm) used in our experiments, d_R ranges from ≈ 1 mm for the porcelains down to ≈ 250 μm for the dense zirconia.

An alternative way of assessing the prospective survival of ceramic-based bilayers is illustrated in Figure 7. This figure is constructed for monolithic dental ceramics[46,47] (E_c from Table I) on dentin supports ($E_s = 16$ GPa), in contact with opposing tooth enamel ($E_i = 94$ GPa), with like cuspal radii ($r_i \approx r_c$), at operational load $P_m = 100$ N. Once this information is inserted into Eq. (1), Eqs. (2)–(4) may then be employed to determine critical dimensions for the different damage modes: r_C [cone cracking, $P_C = P_m$ in Eq. (2)], r_Y [quasiplasticity, $P_Y = P_m$ in Eq. (3)], and d_R [radial cracking, $P_R = P_m$ in Eq. (4)]. The design goal is to ensure that these critical dimensions do not exceed the dimensions that define the crown configuration—that is, that r_C and r_Y remain below a minimum cuspal radius (nominal 2–4 mm) and d_R remains

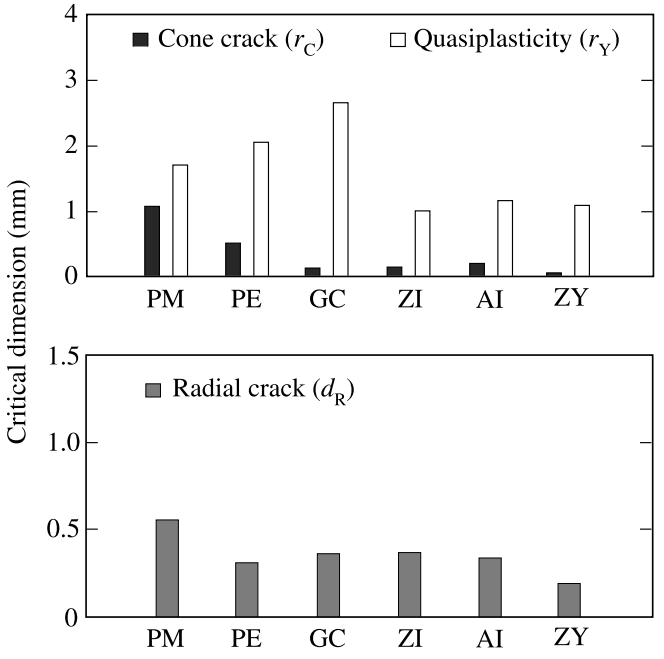

Figure 7. Plots of critical contact radius r_C for cone cracking and r_Y for quasiplasticity, and critical ceramic-layer thickness d_R for radial cracking, at nominal contact force $P = 100$ N. Data for selected dental ceramics: PM, porcelain (Mark II); PE, porcelain (Empress); GC, glass–ceramic (Empress II); ZI, zirconia (glass-infiltrated); AI, alumina (glass infiltrated); ZY, zirconia (Y-TZP).

below a minimum ceramic-layer thickness (nominal 1.0–1.5 mm). It would appear from Figure 7 that most ceramics are relatively immune to cone or radial cracking, provided the contacts do not become unduly sharp or the ceramic layers unduly thin. However, most ceramics (especially the glass–ceramics) are somewhat susceptible to quasiplasticity,[31] because of their relatively low hardness (Table I).

DISCUSSION

Testing of model flat bilayers with spherical indenters has been presented as a means of characterizing relative sensitivities of prospective ceramic materials for applications in brittle coating systems. The study has focused on dental ceramics for crowns, but the methodology has general application to all brittle coating systems. It is suggested that Hertzian contact represents a uniquely simple and powerful route to the identification and analysis of critical failure modes in such systems, representative of the basic elements of occlusal contacts in dental function[3] as well as of in-service contacts in other engineering coating applications. Critical damage modes include cone cracking and quasiplasticity in the near-contact region at the ceramic upper surface,[15] and radial cracking below the indenter at the ceramic lower surface.[23] Again, there is little evidence of interfacial delamination in these experiments, despite the weak epoxy adhesive used to bond the coatings to the substrates. Of the modes observed, radial cracking is considered most dangerous, because it can occur at very low loads in thinner coatings, and because the crack arms can spread over long lateral distances relative to the coating thickness.[45] Moreover, because they tend to close up during unloading [e.g. Figure 5(d)], such cracks can be difficult to detect in ordinary top-surface inspections after the event, especially in opaque ceramics. As indicated (e.g., Figure 1), radial cracking is believed a primary cause of failure in all-ceramic crowns.[9]

A feature of the methodology is the availability of explicit, closed-form relations for the various critical loads in terms of routinely measurable material parameters (e.g., Table I). These relations enable quantitative a priori predictions, with an accuracy of better than a factor of about 2 [2,23]—more than adequate to account for the basic experimental dependencies on coating thickness over the typical data range (e.g., Figure 6). These same relations enable the determination of critical sphere radii and coating thicknesses for the onset of damage in potential dental ceramic/dentin bilayer systems subject to some nominal biting force (e.g., Figure 7, $P_m = 100$ N). The goal is to keep these critical dimensions as small as possible relative to the dimensions that characterize occlusal function: by ensuring sufficiently large cuspal contact radii, so as to avoid cone cracking ($r > r_C$) and quasiplasticity ($r > r_Y$); and by ensuring sufficiently large crown layer thicknesses to avoid radial cracking ($d > d_R$).

Diagrams of the kind shown in Figures 6 and 7 can be useful in rating ceramic materials. Thus it is apparent that porcelains are most susceptible to fracture, and Y-TZP zirconia least susceptible. The fact that porcelain has good aesthetics while Y-TZP does not means that such materials would need to be used in layered combination in order to produce dental crown structures with combined form and function. Dense Y-TZP in particular suggests itself as a particularly attractive candidate as a core ceramic, for its superior strength. It is of interest that the data in Figures 6 and 7 for glass-infiltrated zirconia and alumina core ceramics tend to fall within a common, intermediate group, confirming that the form of the preform material is not a critical factor in the ultimate properties of infiltrated ceramics.[36] This would appear to alleviate the need for unduly stringent quality control in crown core preparation. The glass–ceramic (Empress II) tends to fall within this group, although this material is predicted to be more vulnerable to quasiplasticity. This is because glass–ceramics tend to have weak internal interfaces, hence low hardness (Table I). The especially high vulnerability of the quasiplastic mode to fatigue[20,35,38] and wear [48,49] could contribute to the unacceptably high failure rates of glass–ceramic molar crowns in clinical practice.[24,50]

One aspect of the fracture mechanics relations that bears attention is the dependence of the critical loads on flaw populations in the ceramic layers. Whereas P_C and P_Y in Eqs. (2) and (3) are controlled by flaw-insensitive parameters toughness and hardness, P_R is directly proportional to strength and is therefore susceptible to strength degradation from large flaws. Such susceptibility has been clearly demonstrated in experiments on glass/polycarbonate bilayers containing controlled abrasion[21] or Vickers indentation flaws in

the glass lower surfaces.[45] Flaw statistics can also affect the relation for radial cracking in Eq. (4): The probability of locating a suitably large flaw in the tensile region immediately below the contact diminishes with decreasing coating thickness (owing to lateral spatial scaling with thickness d in the flexure tensile stress field—geometrical similarity), accounting for a nonideal exponent $m < 2$ in the $P_R \propto d^m$ data trends noted in Figure 6.[51] These considerations suggest that ceramics used in crown structures should be prepared with smooth surfaces (especially the undersurfaces), and have fine microstructures, to avoid large flaws. In this context, the common practice of finishing the inner surfaces of some dental crowns with sandblast treatments (to remove any surplus glass from infiltration investment processes and to roughen the surfaces for ensuing adhesion to the remnant tooth) could perhaps be reviewed.

The next step in the development of design strategies for dental crowns or other biomedical multilayer structures would appear to be to obtain analytical relations analogous to Eq. (4) for radial cracking in flat all-ceramic veneer/core crowns on soft dentinlike substrates, that is, trilayers[25] [assuming the critical loads for cone cracking and quasiplasticity in Eqs. (1) and (2) remain reasonable approximations]. What combinations of material properties and layer thicknesses offer maximum resistance to lifetime-threatening damage? Once this question is answered, incorporation of more complex geometrical shapes into detailed engineering-based models that characterize actual crown configurations may be contemplated.

Thanks are due to H. W. Kim, Y. W. Rhee, I. M. Peterson, J. Quinn, and H. Xu for providing some of the data in Table I. Specimen materials were generously supplied by H. Hornberger of Vita Zahnfabrik, Bad Sackingen, Germany, and E. Levadnuk of Norton Desmarquest Fine Ceramics, East Granby, CT.

REFERENCES

1. Lawn BR. Indentation of ceramics with spheres: A century after Hertz. J Am Ceram Soc 1998;81:1977–1994.
2. Lawn BR et al. Damage-resistant brittle coatings. Adv Eng Mater 2000;2:745–748.
3. DeLong R, Douglas WH. Development of an artificial oral environment for the testing of dental restoratives: Bi-axial force and movement control. J Dent Res 1983;62:32–36.
4. Scherrer SS, Rijk WG. The fracture resistance of all-ceramic crowns on supporting structures with different elastic moduli. Int J Prosthodont 1993;6:462–467.
5. Scherrer SS, Rijk WG, Belser UC, Meyer JM. Effect of cement film thickness on the fracture resistance of a machinable glass–ceramic. Dent Mater 1994;10:172–177.
6. Kelly JR. Ceramics in restorative and prosthetic dentistry. Annu Rev Mater Sci 1997;27:443–468.
7. Peterson IM, Pajares A, Lawn BR, Thompson VP, Rekow ED. Mechanical characterization of dental ceramics using Hertzian contacts. J Dent Res 1998;77:589–602.
8. Tsai YL, Petsche PE, Yang MC, Anusavice KJ. Influence of glass–ceramic thickness on Hertzian and bulk fracture mechanisms. Int J Prosthodont 1998;11:27–32.
9. Kelly JR. Clinically relevant approach to failure testing of all-ceramic restorations. J Prosthet Dent 1999;81:652–661.
10. Frank FC, Lawn BR. On the theory of Hertzian fracture. Proc R Soc London Ser A 1967;299:291–306.
11. Lawn BR, Wilshaw TR. Indentation fracture: Principles and applications. J Mater Sci 1975;10:1049–1081.
12. Lawn BR. Fracture of brittle solids. Cambridge: Cambridge University Press; 1993.
13. Lawn BR, Padture NP, Cai H, Guiberteau F. Making ceramics 'ductile'. Science 1994;263:1114–1116.
14. Guiberteau F, Padture NP, Cai H, Lawn BR. Indentation Fatigue: A simple cyclic Hertzian test for measuring damage accumulation in polycrystalline ceramics. Philos Mag 1993;68:1003–1016.
15. Rhee YW, Kim HW, Deng Y, Lawn BR. Brittle fracture versus quasiplasticity in ceramics: A simple predictive index. J Am Ceram Soc 2001;84:561–565.
16. An L, Chan HM, Padture NP, Lawn BR. Damage-resistant alumina-based layer composites. J Mater Res 1996;11:204–210.
17. Wuttiphan S, Lawn BR, Padture NP. Crack suppression in strongly-bonded homogeneous/heterogeneous laminates: A study on glass/glass–ceramic bilayers. J Am Ceram Soc 1996;79:634–640.
18. Chan HM. Layered ceramics: Processing and mechanical behavior. Annu Rev Mater Sci 1997;27:249–282.
19. Lee KS, Wuttiphan S, Hu XZ, Lee SK, Lawn BR. Contact-induced transverse fractures in brittle layers on soft substrates: A study on silicon nitride bilayers. J Am Ceram Soc 1998;81:571–580.
20. Jung YG, Wuttiphan S, Peterson IM, Lawn BR. Damage modes in dental layer structures. J. Dent Res 1999;78:887–897.
21. Chai H, Lawn BR, Wuttiphan S. Fracture modes in brittle coatings with large interlayer modulus mismatch. J Mater Res 1999;14:3805–3817.
22. Chai H, Lawn BR. Role of adhesive interlayer in transverse fracture of brittle layer structures. J Mater Res 2000;15:1017–1024.
23. Rhee Y-W, Kim HW, Deng Y, Lawn BR. Contact-induced damage in ceramic coatings on compliant substrates: fracture mechanics and design. J Am Ceram Soc 2001;18:1066–1072.
24. Malament KA, Socransky SS. Survival of Dicor glass–ceramic dental restorations over 14 years: I. Survival of Dicor complete coverage restorations and effect of internal surface acid etching, tooth position, gender and age. J Prosthet Dent. 1999;81:23–32.
25. Miranda P, Pajares A, Guiberteau F, Cumbrera FL, Lawn BR. Contact fracture of brittle bilayer coatings on soft substrates. J Mater Res 2001;16:115–126.
26. Cai H, Kalceff MAS., Lawn BR. Deformation and fracture of mica-containing glass–ceramics in Hertzian contacts. J Mater Res 1994;9:762–770.
27. Guiberteau F, Padture NP, Lawn BR. Effect of grain size on Hertzian contact in alumina. J Am Ceram Soc 1994;77:1825–1831.
28. Cai H, Kalceff MAS, Hooks BM, Lawn BR, Chyung K. Cyclic fatigue of a mica-containing glass–ceramic at Hertzian contacts. J Mater Res 1994;9:2654–2661.
29. Lee SK, Lawn BR. Contact fatigue in silicon nitride. J Am Ceram Soc 1999;82:1281–1288.
30. Chyung CK, Beall GH, Grossman DG. Microstructures and mechanical properties of mica glass–ceramics. In: Thomas G, Fulrath RM, Fisher RM, editors. Electron microscopy and structure of materials. Berkeley, CA: University of California Press; 1972. p 1167–1194.
31. Peterson IM, Wuttiphan S, Lawn BR, Chyung K. Role of microstructure on contact damage and strength degradation of micaceous glass–ceramics. Dent Mater 1998;14:80–89.
32. Grossman DG. Structure and physical properties of Dicor/MGC glass–ceramic. In: Mörmann WH, editor. Proceedings of the

International Symposium on Computer Restorations. Chicago, IL: Quintessence; 1991. p 103–115.
33. Jung YG, Peterson IM, Kim DK, Lawn BR. Lifetime-limiting strength degradation from contact fatigue in dental ceramics. J Dent Res 2000;79:722–731.
34. Lawn BR, Lee SK, Peterson IM, Wuttiphan S. A model of strength degradation from Hertzian contact damage in tough ceramics. J Am Ceram Soc 1998;81:1509–1520.
35. Kim DK, Jung YG, Peterson IM, Lawn BR. Cyclic fatigue of intrinsically brittle ceramics in contact with spheres. Acta Mater 1999;47:4711–4725.
36. Jung YG, Peterson IM, Pajares A, Lawn BR. Contact damage resistance and strength degradation of glass-infiltrated alumina and spinel ceramics. J Dent Res 1999;78:804–814.
37. Yeo JG, Lee KS, Lawn BR. Role of microstructure in dynamic fatigue of glass–ceramics after contact with spheres. J Am Ceram Soc 2000;83:1545–1547.
38. Lee KS, Jung YG, Peterson IM, Lawn BR, Kim DK, Lee SK. Model for cyclic fatigue of quasiplastic ceramics in contact with spheres. J Am Ceram Soc 2000;83:2255–2262.
39. White SN, Zhao XY, Yu Z, Li ZC. Cyclic mechanical fatigue of a feldspathic dental porcelain. Int J Prosthodont 1995;8:413–420.
40. Fischer-Cripps AC, Lawn BR, Pajares A, Wei L. Stress analysis of elastic–plastic contact damage in ceramic coatings on metal substrates. J Am Ceram Soc 1996;79:2619–2625.
41. Lee KS, Rhee YW, Blackburn DH, Lawn BR, Chai H. Cracking of brittle coatings adhesively bonded to substrates of unlike modulus. J Mater Res 2000;15:1653–1656.
42. Tabor D. Hardness of metals. Oxford: Clarendon; 1951
43. McColm IJ. Ceramic hardness. New York: Plenum; 1990
44. Anstis GR, Chantikul P, Marshall DB, Lawn BR. A critical evaluation of indentation techniques for measuring fracture toughness: I. Direct crack measurements. J Am Ceram Soc 1981;64:533–538.
45. Kim HW, Deng Y, Miranda P, Pajaver A, Kim DK, Kim HE, Lawn BR. Effect of flaw state on the strength of brittle coatings on soft substrates. J Am Ceram Soc 2001;84:2377–2384.
46. Xu HHK, Smith DT, Jahanmir S, Romberg E, Kelley JR, Thompson VP. Indentation damage and mechanical properties of human enamel and dentin. J Dent Res 1998;77:472–480.
47. Kinney NH, Balooch M, Marshall GM, Marshall SJ. A micromechanics model of the elastic properties of human dentine. Arch Oral Biol 1999;44:813–822.
48. Xu HHK, Smith DT, Jahanmir S. Influence of microstructure on indentation and machining of dental glass–ceramics. J Mater Res 1996;11:2325–2337.
49. Nagarajan VS, Jahanmir S. Relationship between microstructure and wear of mica-containing glass–ceramics. Wear 1996; 200:176–185.
50. Sjogren G, Lantto R, Tillberg A. Clinical evaluation of all-ceramic crowns (Dicor) in general practice. J. Prosthet. Dent. 1999;81:277–284.
51. Miranda P, Pajares A, Guiberteau F, Cumbrera FL, Lawn BR. Role of flaw statistics in contact fracture of brittle coatings. Acta Mater 2001;49:3719–3726.